

## AM1 and Single-crystal X-ray Diffraction Study of the Conformational Properties of Chlorinated Diphenyl Ethers

Tapio Nevalainen<sup>a</sup> and Kari Rissanen<sup>b</sup>

<sup>a</sup> Department of Chemistry, University of Jyväskylä, PO Box 35, FIN-40351, Jyväskylä, Finland

<sup>b</sup> Department of Chemistry, University of Joensuu, PO Box 111, FIN-80101, Joensuu, Finland

Structural and conformational properties of 11 polychlorinated diphenyl ethers (PCDEs) 1–11 and thyroxine derivative 12 were studied by the semiempirical AM1 method. In addition, the molecular structures of six PCDEs 1–6 were solved by X-ray crystallography. Conformational analyses for diphenyl ethers 1–12 were performed and the resulting conformational energy maps obtained. The calculated energy minima of PCDEs were obtained, and the structural parameters were compared with the X-ray structures. The X-ray-determined geometries were found to be inside the low-energy regions close to the global energy minima except for compound 2, whose X-ray structure deviates considerably from the global minima. The X-ray structures of PCDE were non-planar, with dihedral angles between two benzene rings ranging from 59.0° to 99.7°.

It seems that polychlorinated diphenyl ethers (PCDEs) are being considered more and more as potentially dangerous environmental contaminants, which have been found in fish, birds and humans.<sup>1–3</sup> The PCDEs have been shown to have toxic properties similar to those of polychlorinated biphenyls (PCBs).<sup>4</sup> The toxic equivalence factors (TEFs) proposed by Safe<sup>5</sup> for non- and mono-*ortho*-substituted PCDEs (TEFs = 0.001) are the same as for mono-*ortho* coplanar PCBs. According to the toxicity study by Howie *et al.*<sup>6</sup> PCDEs 2 and 4 (Fig. 1) showed the highest immunosuppressive induction activities of eight PCDEs studied (ED<sub>50</sub> values 0.5 and 0.7 μmol kg<sup>-1</sup>, respectively). The activities of isomers 1 (258 μmol kg<sup>-1</sup>) and 7 (50.6 μmol kg<sup>-1</sup>) were very low. The toxicities of the other PCDEs studied here are still unknown.

There are four possible conformations of diphenyl ethers involved in the conformational equilibrium: planar ( $\varphi_1 = \varphi_2 = 0^\circ$ ), 'butterfly' ( $\varphi_1 = \varphi_2 = 90^\circ$ ), skew ( $\varphi_1 = 0^\circ$ ,  $\varphi_2 = 90^\circ$ ) and twist ( $\varphi_1, \varphi_2 > 0^\circ$ ), in which  $\varphi_1$  and  $\varphi_2$  are defined as dihedral angles between the C–O–C plane and the two-ring planes. Experiments and theoretical calculations have shown that diphenyl ethers adopt a twist or skew conformation depending on the number of *ortho* substituents.<sup>7–9</sup> Previous crystal structure studies on 3,3',4,4'-tetrachlorodiphenyl ether<sup>10</sup> (7), 2,2',4,4'-tetrachlorodiphenyl ether<sup>11</sup> (8) and 2,2',3,4,4',5'-hexachlorodiphenyl ether<sup>12</sup> (9) showed that 7 and 8 adopt the twist conformation and 9 adopts a conformation close to the skew form. Preference for the twist or skew conformation is a result of competing forces: (a) the tendency of each phenyl ring to prefer a plane perpendicular to the two lone-pairs of electrons on oxygen so that conjugation between oxygen and the ring may take place; and (b) steric repulsion among the four *ortho* substituents and the  $\pi$ -cloud of the rings. Conjugation alone makes a planar conformation lowest in energy while steric factors alone favour a more 'butterfly' conformation.

In the present work, a semiempirical AM1 method<sup>13</sup> was utilized in calculating the conformational properties of PCDEs together with X-ray structure determination of six new PCDEs. The objective of this work was to investigate the effect of *ortho*-chlorine substituents on the rotation of phenyl rings and to compare the calculated conformations with the X-ray structures. Results of conformational analyses of the PCDE isomers are presented as conformational energy maps. Based upon these maps, the number and location of conformational minima and their relative energies can be found. These maps give the height

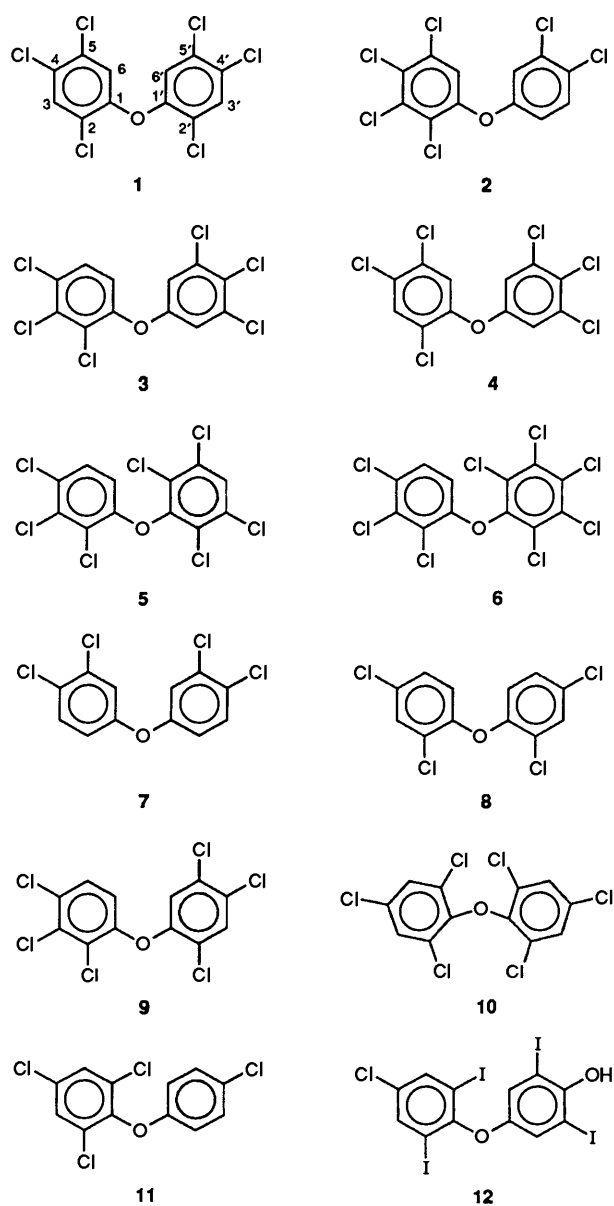
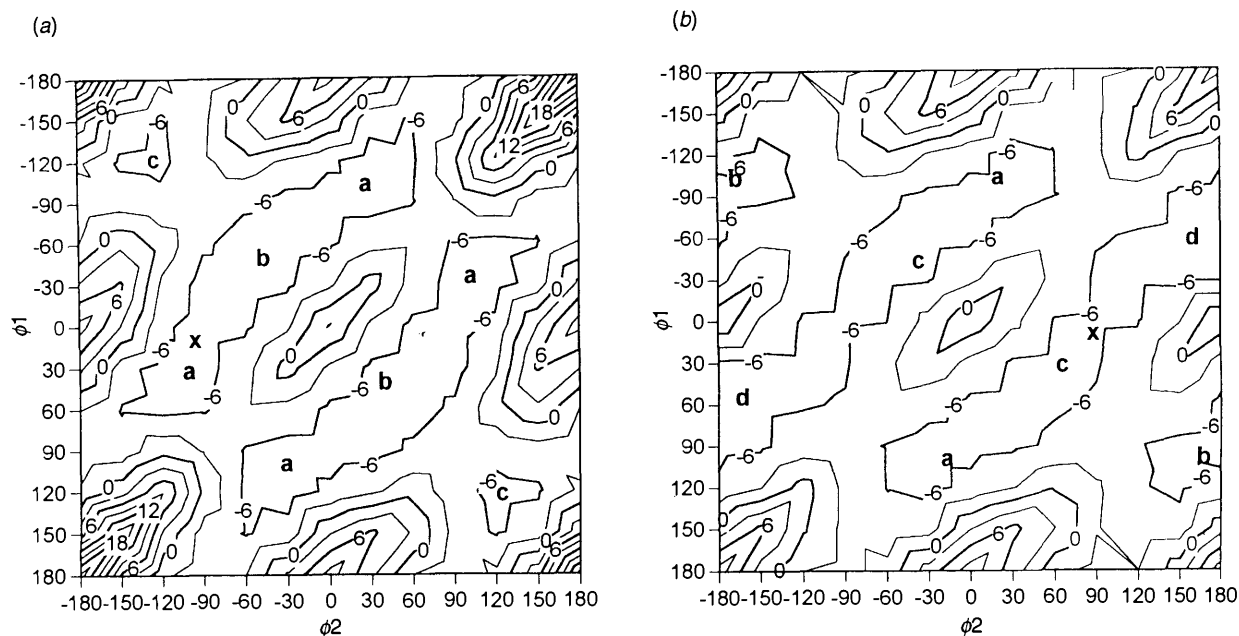
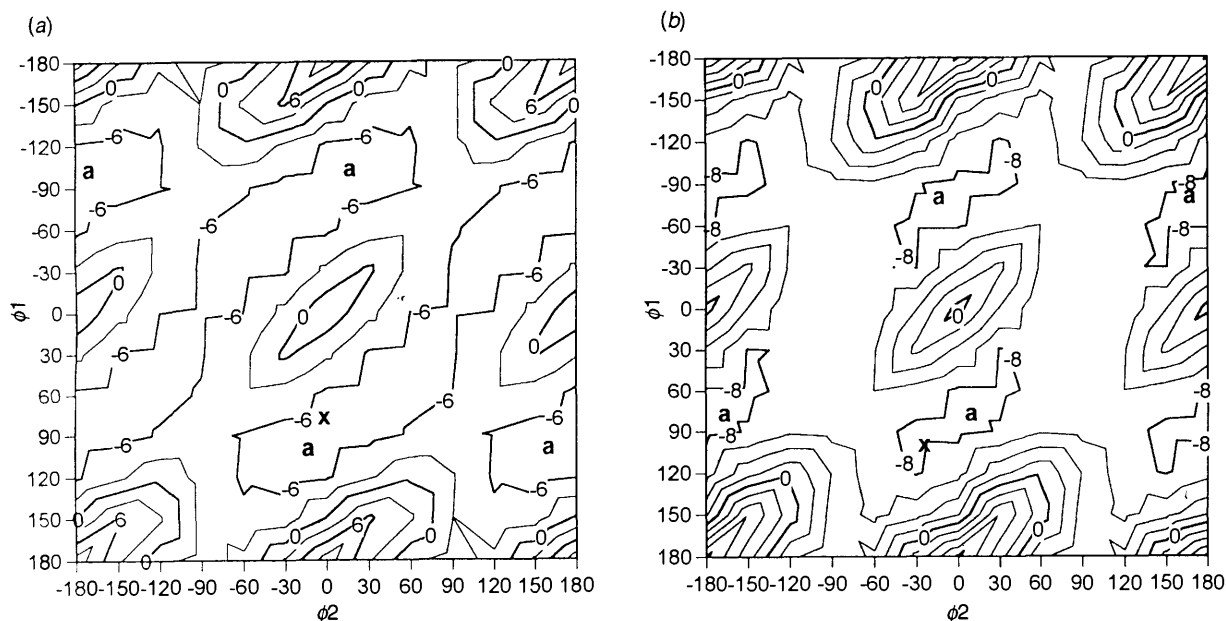


Fig. 1 Numbering and the (planar) starting conformations ( $\varphi_1 = \varphi_2 = 0^\circ$ ) of diphenyl ethers 1–12



**Fig. 2** (a) Conformational energy map for PCDE 1 as functions of two dihedral angles:  $\phi_1$  and  $\phi_2$ . (b) Conformational energy map for PCDE 2. Contours are drawn every 3.0 kcal mol<sup>-1</sup>. **a** labels global minima and **b**, **c** and **d** local minima. **x** labels the position of X-ray structure.



**Fig. 3** (a) Conformational energy map for PCDE 3 (contours 3.0 kcal mol<sup>-1</sup>) and (b) for PCDE 4 (contours 2.0 kcal mol<sup>-1</sup>)

of internal rotation barriers and the size of the low-energy regions around the minima. The interconversion between the energy minima in diphenyl ether type compounds may occur by a disrotatory mechanism *via* the skew transition state ( $\phi_1 = 0^\circ$ ,  $\phi_2 = 90^\circ$ ) or by a conrotatory mechanism *via* the 'butterfly' ( $\phi_1 = \phi_2 = 90^\circ$ ) transition state.<sup>7</sup>

### Results and Discussion

The conformations of diphenyl ethers are described in terms of the torsion angles  $\phi_1 = [\text{C}(6)-\text{C}(1)-\text{O}-\text{C}(1')]$  and  $\phi_2 = [\text{C}(6')-\text{C}(1')-\text{O}-\text{C}(1)]$  (Fig. 1). The dihedral angles  $\phi_1$  and  $\phi_2$  are defined as positive when the rotation is clockwise looking down the  $\text{C}(4)-\text{C}(1)$  and  $\text{C}(4')-\text{C}(1')$  axes toward the oxygen. The starting structures ( $\phi_1 = \phi_2 = 0^\circ$ ) in the conformational maps are the same as shown in Fig. 1.

Figs. 2–7 show the AM1 conformational energy maps for diphenyl ethers 1–12 as functions of the dihedral angles:  $\phi_1$  and

$\phi_2$ . The AM1 calculated heats of formation and the corresponding dihedral angles of calculated minimum conformers and the X-ray structures are presented in Table 1.

Non-*ortho*-isomer 7 has three different energy minima **a**, **b** and **c** [Table 1 and Fig. 5(a)]. The conformation of global minimum energy (**a**) was found at  $\phi_1 = \phi_2 = 38^\circ$ , whereas the X-ray structure was found near the minima at  $\phi_1 = 59.1^\circ$ ,  $\phi_2 = 25.5^\circ$ . The corresponding conformation for the unsubstituted diphenyl ether calculated by the AM1 method appears at  $\phi_1 = \phi_2 = 37^\circ$ . In previous conformational analyses on diphenyl ether, the minimum energy conformation was located at  $\phi_1 = \phi_2 = 35^\circ$ , calculated by the semiempirical C-INDO method.<sup>9</sup>

The conformational energy map of 7 [Fig. 5(a)] reveals that a very large region of the conformational space is energetically allowed, so that the molecular population becomes distributed over a wide range of torsional angles at ordinary temperatures. The rotational barriers separating conformational minima are

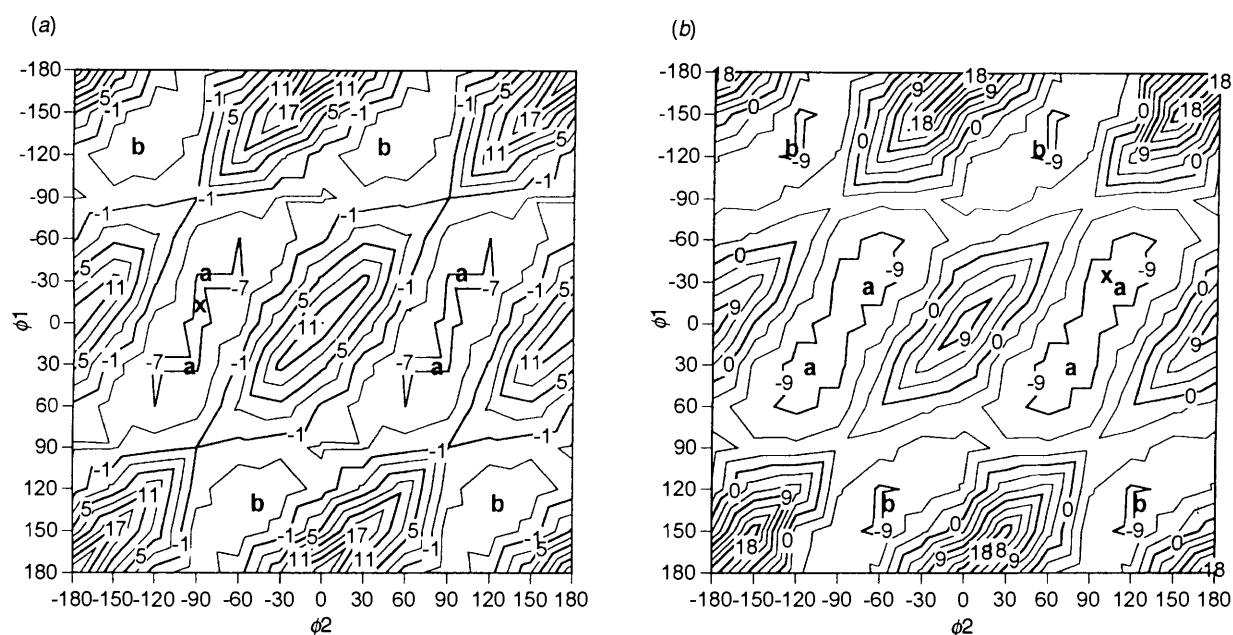


Fig. 4 (a) Conformational energy map for PCDE 5 (contours 3.0 kcal mol<sup>-1</sup>) and (b) for PCDE 6 (contours 3.0 kcal mol<sup>-1</sup>)

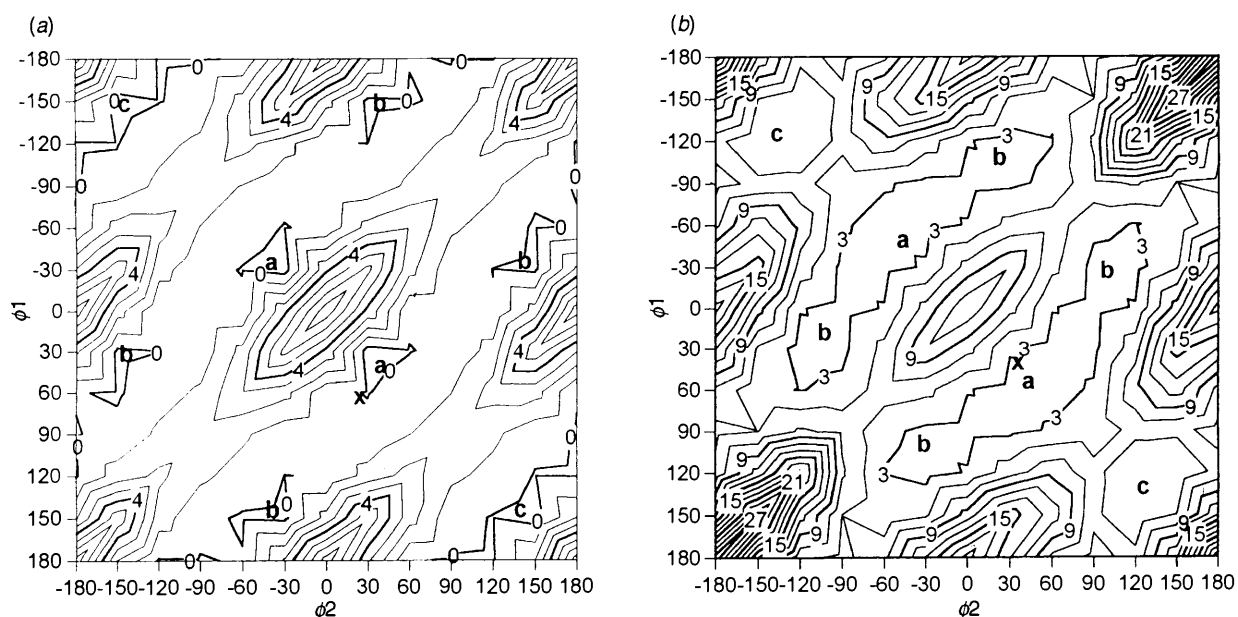


Fig. 5 (a) Conformational energy map for PCDE 7 (contours 1.0 kcal mol<sup>-1</sup>) and (b) for PCDE 8 (contours 2.0 kcal mol<sup>-1</sup>)

below 0.5 kcal mol<sup>-1</sup>, which means that the free molecule can pass continuously from one energy minimum to another at room temperature.

Single *ortho*-chlorinated PCDEs 2 [Fig. 2(b)], 3 [Fig. 3(a)] and 4 [Fig. 3(b)] have large low-energy regions, where the two rings may oscillate between a wide range of torsion angles (110°, -30°) and (-110°, -150°). The X-ray-determined geometry of compound 2 adopts a conformation close to the skew form (6.9°, 78.8°). It deviates considerably from the global energy minima **a** (105°, -18°) but is located near the local minima **c** [Fig. 2(b)]. The X-ray conformation of 2 is 0.54 kcal mol<sup>-1</sup> higher in energy (calculated using the X-ray-determined torsion angles) than the AM1-optimized global minima. The X-ray structures of 3 and 4 lie inside the 0.3 kcal mol<sup>-1</sup> contour around the global minima (Fig. 3). Barriers to internal rotation in 2-4 are low (<1 kcal mol<sup>-1</sup>), so the conformers can easily interconvert *via* skew conformations at (0°, ±90°), (±90°, 0°) and (±90°, 180°).

The conformational maps of 2,2'-di-*ortho* isomers 1 [Fig. 2(a)], 8 [Fig. 5(b)] and 9 [Fig. 6(a)] look very similar. There is a very shallow low-energy region between the dihedral angles (120°, -60°) and (-60°, 120°). The barriers to rotation between the energy minima *via* the (0°, ±90°) and (±90°, 0°) transition conformations are very low (<0.5 kcal mol<sup>-1</sup>). There are also local energy minima at  $\phi_1 = \phi_2 = 131-135^\circ$  where the lowest energy path goes through the butterfly (90°, 90°) transition state, the rotational barrier being about 1.5 kcal mol<sup>-1</sup>. The interconversion barrier through the skew form (±90°, 180°) is about 2.2 kcal mol<sup>-1</sup> for 1, 8 and 9. The calculated global energy minima for compounds 1 (105°, -29°) and 9 (111°, -27°) are close to each other, but they differ from that of compound 8 (45°, 45°) because of the absence of chlorines at the *meta* position. The X-ray structure of 8 (-34.2°, -34.2°) also differs from the corresponding structures of 1 (-106.1°, 16.6°) and 9 (95.3°, 0.3°).

Triply *ortho*-substituted PCDEs 5 [Fig. 4(a)] and 6 [Fig.

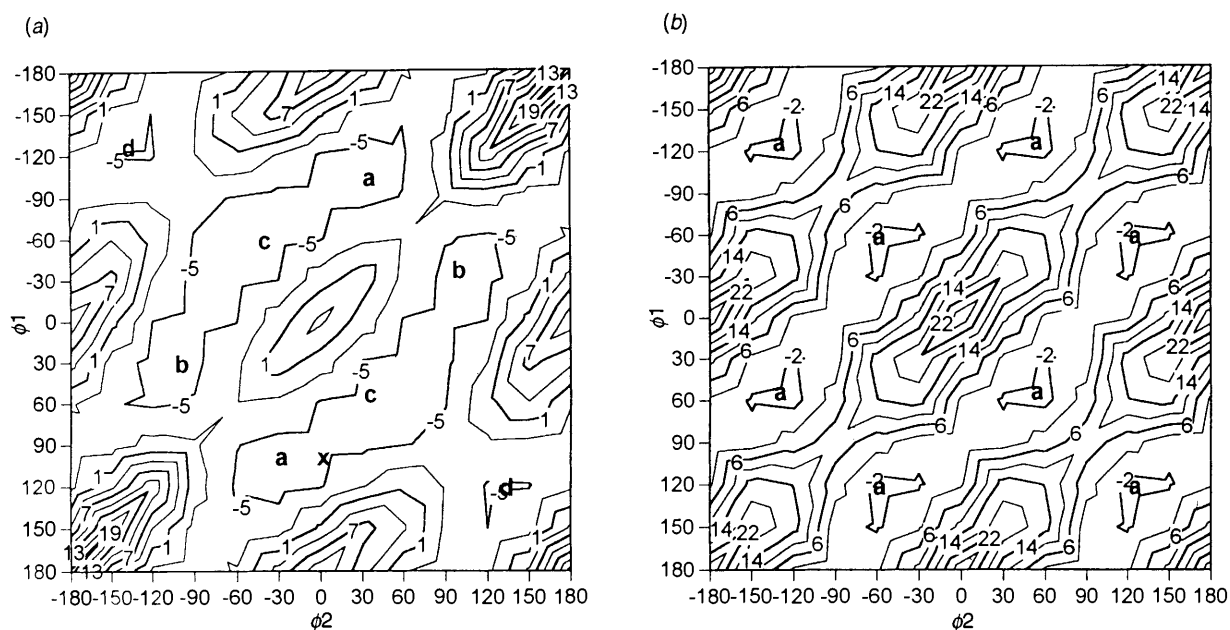


Fig. 6 (a) Conformational energy map for PCDE 9 (contours 3.0 kcal mol<sup>-1</sup>) and (b) for PCDE 10 (contours 4.0 kcal mol<sup>-1</sup>)

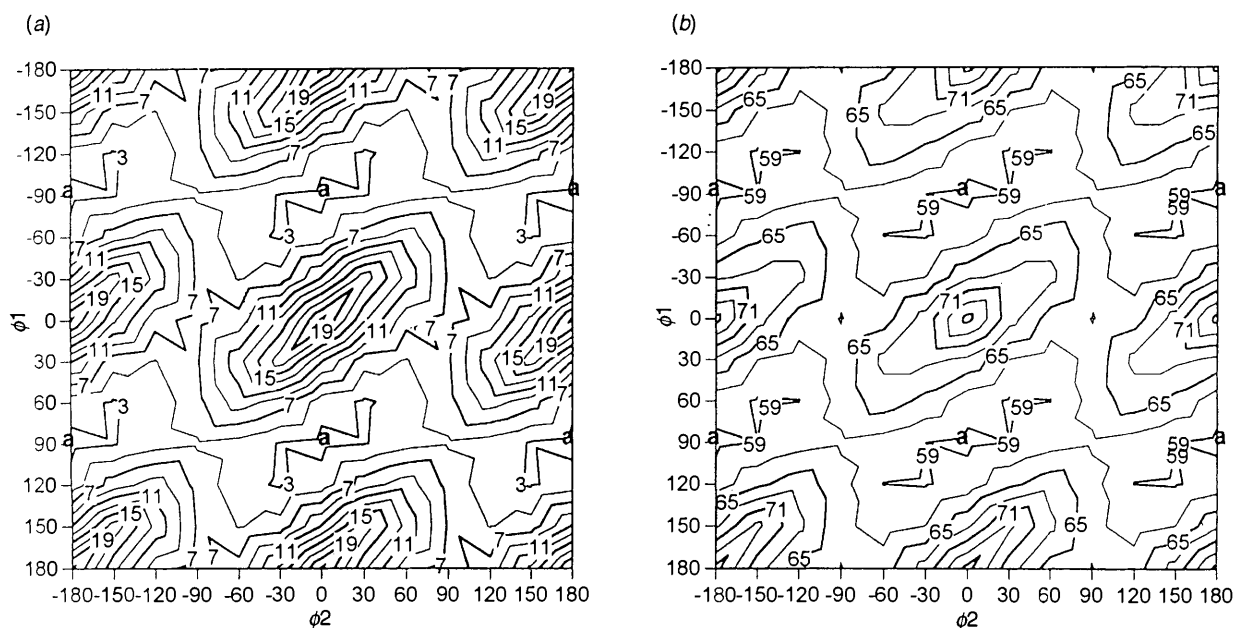


Fig. 7 (a) Conformational energy map for PCDE 11 (contours 2 kcal mol<sup>-1</sup>) and (b) for thyroxine derivative 12 (contours 3 kcal mol<sup>-1</sup>)

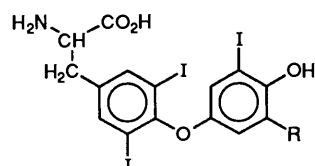


Fig. 8 Thyroid hormone structures: thyroxine (T4), R = I, and 3,5,3'-triiodothyronine (T3), R = H

4(b)] have a low-energy region around the line between (60°, -120°) and (-60°, -60°), containing two identical energy minima. The barriers between these two equivalent minima (a) are only 0.13 kcal mol<sup>-1</sup>. The barrier to rotation between the local minima b (Fig. 4) and global minima a is about 3.5 kcal mol<sup>-1</sup> through the lowest skew (90°, 0°) transition state.

Tetra-ortho-isomer 10 [Fig. 6(b)] has one torsional energy minimum, and the barrier through the lowest skew (90°, 0°)

transition state between these identical minima is only about 2 kcal mol<sup>-1</sup>. The interconversion barrier through the butterfly (90°, 90°) transition state is almost 12 kcal mol<sup>-1</sup>.

2,6-Di-ortho ethers 11 [Fig. 7(a)] and 12 [Fig. 7(b)] exhibit a single minimum that has a skew conformation (0°, 90°) and the rotation occurs *via* the conrotatory mechanism (through  $\phi_1 = \phi_2 = 90^\circ$  transition state). The motional behaviour of PCDE 11 is similar to that of thyroid hormones: thyroxine (T4) and 3,5,3'-triiodothyronine (T3) (Fig. 8).

The structure of thyroxine in the conformational analysis is replaced by thyroxine analogue 12, where the alanine side chain is left out on the presumption that it is too far away from the ether linkage to significantly affect the conformational properties. The rotational barriers between the minima (through  $\phi_1 = \phi_2 = 90^\circ$  transition state) are 2.4 kcal mol<sup>-1</sup> for 11 and 3.2 kcal mol<sup>-1</sup> for 12. In an earlier CNDO/2 study by Kollman *et al.*<sup>14</sup> the rotational barrier for 2,6-diiododiphenyl ether was 15.5 kcal mol<sup>-1</sup>, and for the 2,6-dichloridiphenyl ether

**Table 1** Calculated heats of formation ( $\Delta H_f$ ) and their corresponding torsion angles  $\varphi_1 = [C(6)-C(1)-O-C(1')]$  and  $\varphi_2 = [C(6')-C(1')-O-C(1)]$  for AM1-calculated minimum energy conformations (see Figs. 2-7) and for X-ray structures<sup>a</sup>

Compound	Conformer	$\Delta H_f/\text{kcal mol}^{-1}$	$\varphi_1(^{\circ})$	$\varphi_2(^{\circ})$
1	a	-7.42	$\pm 29 (\pm 105)$	$\pm 105 (\pm 29)$
	b	-7.28	$\pm 44$	$\pm 44$
	c	-6.83	$\pm 135$	$\pm 135$
	X-Ray	-7.38	-106.1	16.6
2	a	-7.02	$\pm 105$	$\pm 18$
	b	-6.91	$\pm 108$	$\pm 162$
	c	-6.79	$\pm 32$	$\pm 48$
	d	-6.76	$\pm 56$	$\pm 162$
	X-Ray	-6.49	6.9	78.8
3	a	-7.31	$\pm 104$	$\pm 15 (\pm 165)$
	X-Ray	-7.22	84.7	5.8
4	a	-8.53	$\pm 102$	$\pm 15 (\pm 165)$
	X-Ray	-8.51	112.4	-26.4
5	a	-7.89	$\pm 27$	$\pm 77 (\pm 103)$
	b	-7.17	$\pm 136 (\pm 136)$	$\pm 52 (\pm 128)$
	X-Ray	-7.76	-5.1	-83.2
6	a	-10.66	$\pm 28$	$\pm 76 (\pm 104)$
	b	-9.94	$\pm 133$	$\pm 129 (\pm 51)$
	X-Ray	-10.61	-34.6	103.8
7	a	-0.46	$\pm 38$	$\pm 38$
	b	-0.40	$\pm 39 (\pm 149)$	$\pm 149 (\pm 39)$
	c	-0.29	$\pm 148$	$\pm 148$
	X-Ray	-0.15	59.1	25.5
8	a	2.32	$\pm 45$	$\pm 45$
	b	2.38	$\pm 21 (\pm 107)$	$\pm 107 (\pm 21)$
	c	2.68	$\pm 132$	$\pm 132$
	X-Ray	2.62	-34.2	-34.2
9	a	-6.16	$\pm 111$	$\pm 27$
	b	-6.00	$\pm 31$	$\pm 113$
	c	-5.96	$\pm 57$	$\pm 37$
	d	-5.61	$\pm 131$	$\pm 132$
	X-Ray	-6.03	95.3	0.6
10	a	-3.44	$\pm 56$	$\pm 56 (\pm 124)$
		-3.44	$\pm 124$	$\pm 56 (\pm 124)$
11	a	2.34	$\pm 93$	$\pm 1 (\pm 179)$
12	a	-39.73	$\pm 96$	$\pm 5 (\pm 175)$

<sup>a</sup>  $\Delta H_f$  is calculated using torsion angles taken from X-ray data.

the energy minima were found near 60°, 30°, which based on our results seems to be unreliable.

Bond distances and angles are normal in X-ray structures (Fig. 9) and in the AM1-calculated structures, except that AM1 calculations underestimate the C-Cl bond distance which varies from 1.690 to 1.698 Å, whereas the C-Cl bond lengths in X-ray structures vary from 1.698(6) to 1.748(6) Å. The twist angles (the dihedral angle between mean planes of the two benzene rings) and C-O-C angles between the two benzene rings in PCDEs are presented in Table 2. The C-O-C angles are larger in the crystals than in the calculated structures. The X-ray twist angles between the two benzene rings and the C-O-C angle do not seem to depend on the degree and arrangement of chlorine substitution. It was surprising to observe that di-*ortho* compound **8**, with a symmetrical twist conformation, has an unusually small twist angle, 59°, compared with the near 90° angle in other di-*ortho* compounds.

All the distances between *ortho*-atoms (Table 3) in neighbouring rings are larger than the sum of the van der Waals radii. The shortest distance is found for the X-ray structure of **8**, where the *ortho*-hydrogen distance [H(6)-H(6')] is 2.45 Å (sum of van der Waals radii is 2.4 Å). The shortest AM1 calculated *ortho*-hydrogen distance is found for conformer **7a**, where [H(2)-H(2')] is 2.64 Å.

The conformational energy maps show, that PCDEs are, in general, very flexible molecules, and the barriers between the energy minima are quite low, so that the PCDE structures are not completely rigid even in the tetra-*ortho* case. The X-ray structures are located close to the global energy minima inside

the low-energy area delimited by the 0.3 kcal mol<sup>-1</sup> energy contour. Only the X-ray structure of compound **2** deviates considerably from the global energy minima. This study clearly shows that the conformation of flexible molecules in solid or in other condensed phases is imposed by intermolecular interactions rather than by intramolecular forces. The divergent X-ray structure of isomer **2** and other discrepancies between the X-ray structures and calculated minima are caused by the conformational flexibility of PCDEs that allows isomers to adopt a conformation influenced mainly by the molecule-environment interactions. The discrepancies between X-ray structures and calculated energy minima are smallest in comparatively rigid molecules as in tri-*ortho*-PCDEs **5** and **6**.

This conformational analysis shows that the path for interconversion takes place through the disrotatory mechanism in non-*ortho*, tri-*ortho* and tetra-*ortho*-PCDEs. The conrotatory mechanism is favoured in doubly *ortho*-chlorinated PCDEs.

Toxicity of polychlorinated aromatics is explained by their planar or coplanar geometry with easily polarized substituents in lateral positions.<sup>15</sup> PCDEs differ from other toxic polychloroaromatics in this respect, because planar conformations are strongly disfavoured because of the high energy needed to overcome the *ortho* group repulsion.<sup>8</sup> Because PCDEs structurally resemble thyroid hormones, we can suppose that PCDEs can also bind to the thyroid hormone receptor and function as thyroxine agonists as is shown in the case of 2,3,7,8-tetrachlorodibenzo-*p*-dioxin (TCDD).<sup>16</sup> The high induction activities of PCDEs **2** and **4** can be explained by their having conformational properties similar to thyroid hormones: their

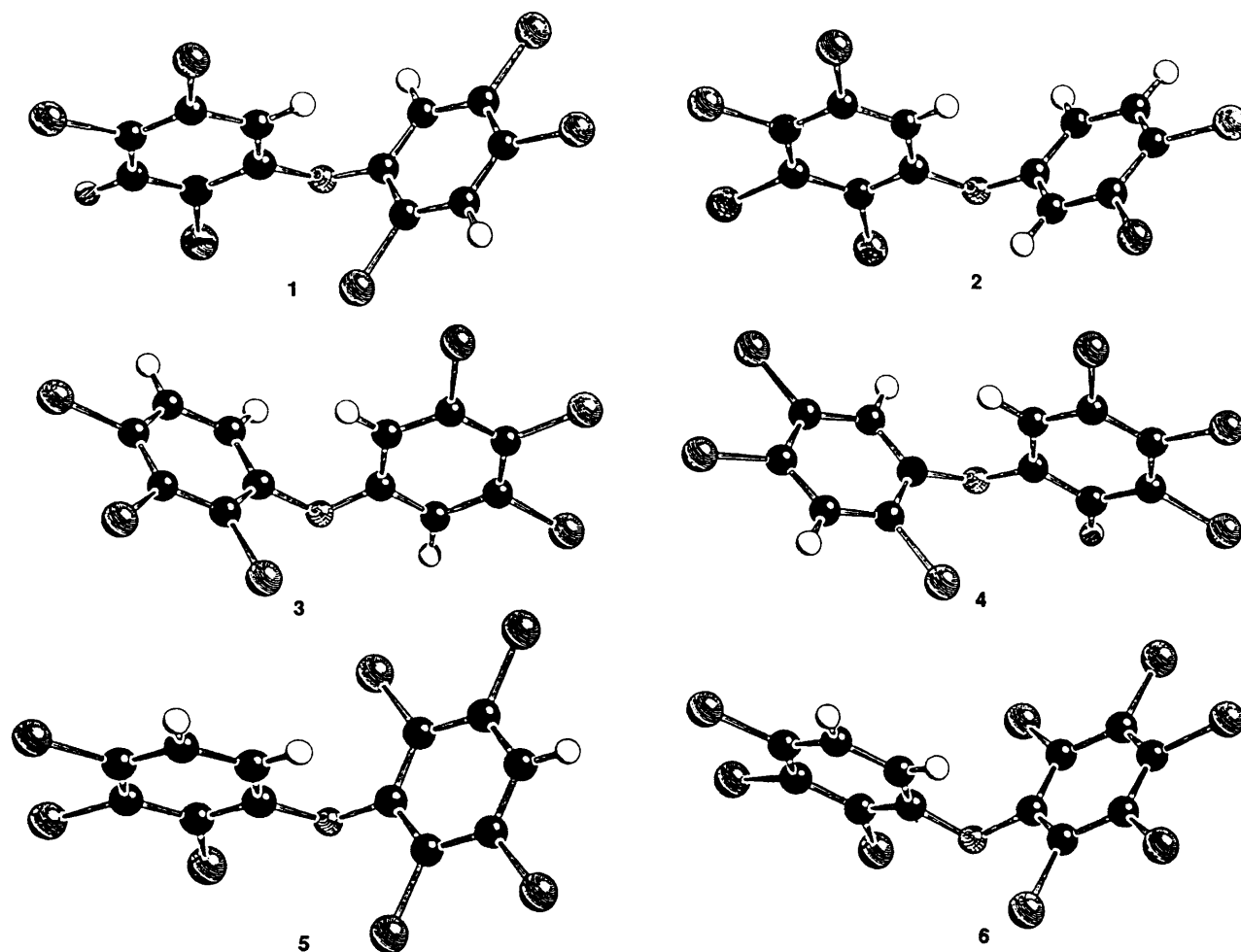
Fig. 9 SCHAKAL<sup>26</sup> plots for compounds 1-6

Table 2 Twist angles (the dihedral angle between mean planes of the two benzene rings) taken from X-ray data and comparison of calculated and observed C-O-C angles

Compound	Chlorine substitution pattern	X-Ray twist angle(°)	C-O-C angle(°)	
			AM1	X-Ray
1	2,2',4,4',5,5'-	97.2	116.0	116.2
2	2,3,3',4,4',5-	99.7	116.3	119.0
3	2,3,3',4,4',5'-	93.6	116.3	118.9
4	2,3',4,4',5,5'-	94.7	116.2	118.3
5	2,2',3,3',4',5,6-	84.0	116.0	118.9
6	2,2',3,3',4,4',5,6-	96.7	115.8	116.5
7	3,3',4,4'-	72.5	117.0	119.6 <sup>11</sup>
8	2,2',4,4'-	59.0	115.6	120.6 <sup>12</sup>
9	2,2',3,4,4',5'-	94.5	116.1	117.2 <sup>13</sup>

energy minima are close to the ( $\pm 90^\circ$ ,  $0^\circ$ ) and ( $\pm 90^\circ$ ,  $180^\circ$ ) conformations. In a QSAR study of PCDEs a correlation has been found between the frontier orbital energy gap and the enzyme induction activities.<sup>17</sup> Combining structural, conformational and electronic properties, we can develop a feasible QSAR model for PCDEs.

### Experimental

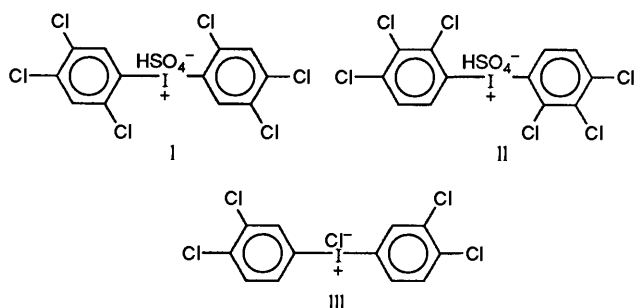
**Compounds.**—PCDEs were synthesized by coupling a biaryliodonium salt with phenol (Table 4).<sup>18</sup> Biaryliodonium salts (I-III) (Fig. 10) were prepared according to Beringer *et al.*<sup>19</sup> by modification of the oxidative coupling of iodyl sulfate with a chlorobenzene. M.p.s (not corrected) were determined with an electrothermal digital-melting-point apparatus model 1A9200.

<sup>1</sup>H NMR spectra were recorded on a JEOL GSX 270, at 270.1 MHz. All chemical shifts are expressed in ppm relative to SiMe<sub>4</sub>. The <sup>1</sup>H NMR data of PCDEs are collected in Table 5. The <sup>13</sup>C NMR spectral data of PCDEs 1, 2, 4-6 have been reported previously.<sup>20</sup>

**Diphenyliodonium salts.** To iodine (6.3 g, 25 mmol), a mixture of conc. H<sub>2</sub>SO<sub>4</sub> (8 cm<sup>3</sup>) and fuming H<sub>2</sub>SO<sub>4</sub> (25%; 15 cm<sup>3</sup>) was added under vigorous stirring. Then a mixture of conc. H<sub>2</sub>SO<sub>4</sub> (2 cm<sup>3</sup>), fuming H<sub>2</sub>SO<sub>4</sub> (25%; 2 cm<sup>3</sup>) and fuming conc. HNO<sub>3</sub> (90%; 4 cm<sup>3</sup>) was slowly added. The mixture was heated at 70-80 °C for 1.5 h, after which yellow iodyl sulfate was precipitated. The iodyl sulfate was then cooled to 0 °C and the chlorobenzene (50 mmol) was slowly added in small portions under vigorous stirring. The mixture was stirred at 50 °C for 3 h and then cooled to 0 °C, and H<sub>2</sub>O (50-100 cm<sup>3</sup>) was carefully added under a

**Table 3** *Ortho*-atom distances for AM1-calculated global minima and for X-ray structures

Conformer	Distance between <i>ortho</i> -atoms/Å			
<b>1 a</b>	3.85 [H(6)–H(6')]	5.29 [H(6)–Cl(2')]	3.21 [Cl(2)–H(6')]	4.40 [Cl(2)–Cl(2')]
X-Ray	3.340	5.016	3.686	4.522
<b>2 a</b>	3.75 [H(6)–H(2')]	4.32 [H(6)–H(6')]	3.29 [Cl(2)–H(2')]	4.81 [Cl(2)–H(6')]
X-Ray	3.045	3.515	4.785	4.902
<b>3 a</b>	3.31 [H(6)–H(6')]	4.78 [H(6)–H(2')]	3.71 [Cl(2)–H(6')]	4.37 [Cl(2)–H(2')]
X-Ray	3.208	4.438	3.705	4.673
<b>4 a</b>	3.24 [H(6)–H(6')]	4.79 [H(6)–H(2')]	3.81 [Cl(2)–H(6')]	4.41 [Cl(2)–H(2')]
X-Ray	3.311	4.919	3.714	3.983
<b>5 a</b>	3.94 [H(6')–Cl(6)]	3.37 [H(6')–Cl(2)]	4.27 [Cl(2')–Cl(6)]	5.45 [Cl(2')–Cl(6)]
X-Ray	3.518	3.751	4.899	4.769
<b>6 a</b>	3.95 [H(6')–Cl(6)]	3.36 [H(6')–Cl(2)]	4.23 [Cl(2')–Cl(6)]	5.47 [Cl(2')–Cl(6)]
X-Ray	4.133	3.209	3.857	5.544
<b>7 a</b>	4.87 [H(6)–H(6')]	4.12 [H(6)–H(2')]	4.12 [H(2)–H(6')]	2.64 [H(2)–H(2')]
X-Ray	4.816	4.104	4.123	2.991
<b>8 a</b>	3.11 [H(6)–H(6')]	4.14 [H(6)–Cl(2')]	4.14 [Cl(2)–H(6)]	5.56 [Cl(2)–C(2')]
X-Ray	2.450	4.643	4.643	4.946
<b>9 a</b>	4.86 [H(6)–H(6')]	5.27 [H(6)–Cl(2')]	3.81 [Cl(2)–H(6')]	4.39 [Cl(2)–Cl(2')]
X-Ray	3.380	4.784	3.506	4.938
<b>10 a</b>	4.39 [Cl(6)–Cl(6')]	3.73 [Cl(6)–Cl(2')]	3.73 [Cl(2)–Cl(6')]	5.63 [Cl(2)–Cl(2')]
<b>11 a</b>	3.68 [Cl(6)–H(6')]	4.67 [Cl(6)–H(2')]	3.67 [Cl(2)–H(6')]	4.71 [Cl(2)–H(2')]
<b>12 a</b>	3.85 [I(6)–H(6')]	4.00 [I(6)–H(2')]	4.89 [I(2)–H(6')]	4.67 [I(2)–H(2')]

**Fig. 10** Diphenyliodonium salts used as starting materials in preparation of PCDEs 1–6**Table 4** Diphenyl ethers synthesized

Isomer	Starting materials:		Yield (%)	M.p./°C
	Salt	Phenol subst.		
<b>1</b>	<b>I</b>	2,4,5-Cl <sub>3</sub>	52	113–115
<b>2</b>	<b>III</b>	2,3,4,5-Cl <sub>4</sub>	82	134–136
<b>3</b>	<b>II</b>	3,4,5-Cl <sub>3</sub>	35	157–158
<b>4</b>	<b>I</b>	3,4,5-Cl <sub>3</sub>	53	104–105
<b>5</b>	<b>II</b>	2,3,5,6-Cl <sub>4</sub>	36	156–157
<b>6</b>	<b>II</b>	2,3,4,5,6-Cl <sub>5</sub>	30	166–167

**Table 5** Proton NMR data for the diphenyl ethers

Isomer	Solvent	<sup>1</sup> H NMR data (J/Hz)
<b>1</b>	CDCl <sub>3</sub>	7.62 (3-H), 7.03 (6-H)
<b>2</b>	CDCl <sub>3</sub>	7.44 (5'-H), 7.15 (2'-H), 7.11 (6-H), 6.90 (6'-H); J <sub>5',6'}</sub> 8.84, J <sub>6',2'}</sub> 2.83
<b>3</b>	[ <sup>2</sup> H <sub>6</sub> ]Acetone	7.80 (5-H), 7.48 (6-H), 7.48 (2'-, 6'-H); J <sub>5,6}</sub> 8.97
<b>4</b>	CDCl <sub>3</sub>	7.70 (3-H), 7.30 (6-H), 7.11 (2'-, 6'-H)
<b>5</b>	CDCl <sub>3</sub>	7.63 (4-H), 7.29 (5-H), 6.36 (6-H); J <sub>5,6}</sub> 9.13
<b>6</b>	[ <sup>2</sup> H <sub>6</sub> ]Acetone	7.63 (5-H), 7.08 (6-H); J <sub>5,6}</sub> 9.05

ventilated hood. Salts **I** and **II** precipitated as hydrogen sulfates and were filtered off, then washed with water and diethyl ether and dried. Salt **III** was a brown oil. The oil was dissolved in methanol and the salt was precipitated from the methanolic solution as a chloride by dropwise addition of conc. HCl. The

crystals were filtered off, washed with methanol and dried. Yields were 30–60%.

**Chlorinated diphenyl ethers.** A mixture of the diphenyliodonium salt, chlorophenol and sodium hydroxide (2.5 mmol each) was refluxed in water for 2 h, and then allowed to cool. The mixture was extracted with diethyl ether, and the ether extract was dried with sodium sulfate and evaporated to dryness. The product was purified by flash chromatography operating with a 2 × 30 cm glass column packed with Kieselgel 60 (230–400 mesh, Merck) and using hexane as eluent.

**Computational Details.**—The semiempirical AM1 molecular orbital calculations were performed with a VAX 4000 computer using the AMPAC program package (QCPE No. 506).<sup>21</sup> The C–C and C–O bond lengths were started at 1.40 Å, C–H bond lengths as 1.10 Å, and C–Cl bond lengths at 1.70 Å. All aromatic bond angles were input at 120°. The conformational analyses were performed on a grid with 30° spacing. The fully relaxed ( $\varphi_1, \varphi_2$ ) maps of the PCDEs are the result of 144 full optimizations of all degrees of freedom except  $\varphi_1$  and  $\varphi_2$ , which were frozen at each grid point. In the case of the symmetrical phenyl ring, fewer optimizations were required to complete a 30° grid. Rotation of symmetrical phenyl ring yielded an equivalent structure, therefore only half the grid points were needed to evaluate an entire map. The ( $\varphi_1, \varphi_2$ ) optimizations were performed using key words AM1, geo-ok,  $T = 40\ 000$ . With the aid of the conformational maps, full geometrical optimizations were performed using the structure at the closest grid point to a possible energy minima. The locations of energy minima of PCDEs and the energies of X-ray structures were calculated with key words: AM1, precise,  $T = 20\ 000$ .

**X-Ray Crystal Structure Analyses of Compounds 1–6.**—Table 6 summarizes the crystal data and refinement parameters. The fractional coordinates with esds in parentheses and equivalent isotropic temperature factors for compounds 1–6 have been deposited at the Cambridge Crystallographic Data Centre\* together with the bond distances (Å) and angles (°). Data were collected from colourless crystals with an Enraf–Nonius CAD-4 diffractometer using graphite monochromatized Cu-K $\alpha$  or Mo-K $\alpha$  radiation. Lp correction and empirical absorption

\* For details of the CCDC deposition scheme, see 'Instructions for Authors (1994)', *J. Chem. Soc., Perkin Trans 2*, 1994, issue 1.

Table 6 Experimental crystallographic data for compounds 1-6

	1	2	3	4	5	6
Formula	$C_{12}H_4OCl_6$	$C_{12}H_4OCl_6$	$C_{12}H_4OCl_6$	$C_{12}H_4OCl_6$	$C_{12}H_3OCl_7$	$C_{12}H_2OCl_8$
$M_f$	376.88	376.88	376.88	376.88	411.33	445.77
$a/\text{\AA}$	9.248(1)	9.832(1)	13.769(2)	8.382(1)	8.944(1)	4.790(1)
$b/\text{\AA}$	9.361(1)	10.958(1)	12.024(1)	9.130(1)	13.490(3)	24.079(3)
$c/\text{\AA}$	9.793(1)	13.339(2)	8.451(1)	10.100(1)	13.209(3)	13.331(1)
$\alpha/^\circ$	114.83(1)	90	90	104.98(1)	90.00	90
$\beta/^\circ$	113.91(1)	97.66(1)	90	107.55(1)	108.06(1)	92.08(1)
$\gamma/^\circ$	81.35(1)	90	90	83.08(1)	90.00	90
$V/\text{\AA}^3$	711.1(1)	1424.3(3)	1399.1(3)	715.9(1)	1515.1(5)	1536.4(4)
$Z$	2	4	4	2	4	4
$d_{calc}/\text{Mg m}^{-3}$	1.760	1.758	1.789	1.748	1.803	1.927
$\mu/\text{mm}^{-1}$	11.22	11.20	11.40	11.40	1.309	1.469
$\lambda/K_\alpha$ (Cu or Mo)	1.5418	1.5418	1.5418	1.5418	0.7107	0.7107
$F(000)$	372	744	744	372	808	872
Space group	$P-1$	$P2_1/c$	$Pna2_1$	$P-1$	$P2_1/c$	$P2_1/n$
Crystal size/mm	$0.22 \times 0.22 \times 0.30$	$0.15 \times 0.20 \times 0.25$	$0.25 \times 0.25 \times 0.35$	$0.18 \times 0.18 \times 0.30$	$0.26 \times 0.27 \times 0.40$	$0.13 \times 0.18 \times 0.23$
$\theta$ range for latt. meas./ $^\circ$	9-14	8-11	6-12	8-14	7-14	8-13
Scan width ( $\omega$ )/ $^\circ$	$0.50 + 0.14 \tan\theta$	$0.55 + 0.14 \tan\theta$	$0.55 + 0.14 \tan\theta$	$0.60 + 0.14 \tan\theta$	$0.48 + 0.35 \tan\theta$	$0.60 + 0.35 \tan\theta$
$\theta$ range/ $^\circ$	2-75	2-65	2-75	2-75	2-25	2-25
$h$ range	0 $\rightarrow$ 11	0 $\rightarrow$ 11	-1 $\rightarrow$ 17	-1 $\rightarrow$ 10	0 $\rightarrow$ 10	0 $\rightarrow$ 5
$k$ range	-11 $\rightarrow$ 11	0 $\rightarrow$ 12	-1 $\rightarrow$ 15	-11 $\rightarrow$ 11	0 $\rightarrow$ 16	0 $\rightarrow$ 28
$l$ range	-12 $\rightarrow$ 12	-15 $\rightarrow$ 15	-1 $\rightarrow$ 10	-12 $\rightarrow$ 12	-15 $\rightarrow$ 15	-15 $\rightarrow$ 15
Variation of std. refl.	<2%	<2.5%	<2%	<1.5%	<2.5%	<2%
Refl. measured	2647	2062	2062	3563	2974	3129
No. unique refl.	2704	2351	1539	2937	2661	2700
Refl. used in refinement	2501	1918	1312	2529	1817	2105
No. param.	172	172	172	172	181	190
Max. in final $\Delta\rho/e \text{\AA}^{-3}$	0.52	0.47	0.35	0.60	0.41	0.32
$R_{int}$	—	0.042	0.032	0.022	0.010	0.012
$R$	0.057	0.054	0.038	0.068	0.037	0.038
$R_w$	0.071	0.067	0.049	0.082	0.031	0.046
Chebyshev coefficients	22.3, 10.1, 15.4	16.2, 2.72, 12.5	11.8, 2.48, 8.69	19.3, 9.49, 12.0	1.97, -6.22, 0.395, -2.57, -0.582	5.35, 0.226, 4.19

$w = w' \times [1.0 - (\Delta F/6 \times \sigma F)^2]$ ; where  $w' = \text{Chebyshev polynomial for } F_c$

<sup>a</sup> The following values are the same for 1-6:  $T/K = 296 \pm 1$ ; number of refl. for latt. meas. = 25; scan method =  $\omega/2\theta$ ; scan speed/ $^\circ \text{ min}^{-1} = 1-7$ ; condition of obs. refl. =  $I > 3.0\sigma(I)$ ; max. shift/error < 0.01.



correction<sup>22</sup> were applied to the data with the following minimum and maximum correction coefficients: 0.709 and 1.233 (1), 0.811 and 1.311 (2), 0.852 and 1.193 (3), 0.868 and 1.365 (4), 0.755 and 1.288 (5), 0.691 and 1.401 (6).

The structures were solved by Direct Methods<sup>23</sup> and subjected to full-matrix refinement,<sup>24</sup> the scattering factors were taken from ref. 25. All non-H atoms were refined anisotropically. The hydrogen atoms were calculated from their idealized positions (C–H distance 1.00 Å) and refined as riding atoms with fixed isotropic temperature factors ( $U = 0.08 \text{ \AA}^2$ ). Crystals of PCDEs for X-ray determination were grown by slow evaporation of a concentrated ethanol solution.

## References

- 1 J. Paasivirta, J. Tarhanen and J. Soikkeli, *Chemosphere*, 1986, **15**, 1429.
- 2 C. J. Stafford, *Chemosphere*, 1983, **12**, 1487.
- 3 D. T. Williams, B. Kennedy and G. L. LeBel, *Chemosphere*, 1991, **23**, 601.
- 4 M. Becker, T. Phillips and S. Safe, *Toxicol. Environ. Chem.*, 1991, **33**, 189.
- 5 S. Safe, *Chemosphere*, 1992, **25**, 61.
- 6 L. Howie, R. Dickerson, D. Davis and S. Safe, *Toxicol. Appl. Pharmacol.*, 1990, **105**, 254.
- 7 H. Benjamins, F. Haque Dar and W. D. Chandler, *Can. J. Chem.*, 1974, **52**, 3297 and refs. cited therein.
- 8 T. Schaefer, G. H. Penner, C. Takeuchi and P. Tseki, *Can. J. Chem.*, 1988, **66**, 1647.
- 9 I. Baraldi, E. Gallinella and F. Momicchioli, *J. Chim. Phys. Phys.-Chim. Biol.*, 1986, **83**, 653.
- 10 P. Singh and J. D. McKinney, *Acta Crystallogr., Sect. B, Struct. Crystallogr.*, 1980, **36**, 210.
- 11 K. Rissanen, J. Valkonen and L. Virkki, *Acta Crystallogr., Sect. C, Cryst. Struct. Commun.*, 1988, **44**, 1644.
- 12 K. Rissanen and L. Virkki, *Acta Crystallogr., Sect. C, Cryst. Struct. Commun.*, 1989, **45**, 1408.
- 13 M. J. S. Dewar, E. F. Zoebish, E. F. Healy and J. J. P. Stewart, *J. Am. Chem. Soc.*, 1985, **107**, 3902.
- 14 P. E. Kollman, J. M. Murray, M. E. Nuss, E. C. Jorgensen and S. Rothenberg, *J. Am. Chem. Soc.*, 1973, **95**, 8518.
- 15 J. McKinney and E. McConnell, *Chlorinated Dioxins and Related Compounds, Impact on the Environment*, eds. O. Hutzinger, R. W. Frei, E. Merian and F. Pocchairs, Pergamon Press, Oxford, 1982, p. 367.
- 16 J. D. McKinney, J. Fawkes, S. Jordan, K. Chae, S. Oatley, R. E. Coleman and W. Briner, *Environ. Health Perspect.*, 1985, **61**, 41.
- 17 T. Nevalainen and E. Kolehmainen, unpublished work.
- 18 C.-A. Nilsson, Å. Norström, M. Hansson and K. Andersson, *Chemosphere*, 1977, **9**, 599.
- 19 F. M. Beringer, R. A. Falk, M. Karniol, G. Masullo, M. Mausner and E. Sommer, *J. Am. Chem. Soc.*, 1969, **81**, 342.
- 20 T. Nevalainen, E. Kolehmainen, M.-L. Säämänen and R. Kauppinen, *Magn. Reson. Chem.*, 1993, **31**, 100.
- 21 QCPE Program No. 506, AMPAC version 2.1.
- 22 N. Walker and D. Stuart, *Acta Crystallogr., Sect. A, Fund. Crystallogr.*, 1983, **39**, 158.
- 23 G. M. Sheldrick, in *Crystallographic Computing 3*, eds. G. M. Sheldrick, C. Krüger and R. Goddard, Oxford University Press, Oxford, 1985, pp. 175–189.
- 24 D. Watkin, J. R. Carruthers and P. W. Betteridge, CRYSTALS, Chemical Crystallography Laboratory, Oxford, 1990.
- 25 *International Tables for X-ray Crystallography*, Kynoch Press, Birmingham, 1974, vol. IV.
- 26 E. Keller, SCHAKAL 88/V16, Kristallographisches Institut der Universität Freiburg, 1990.

Paper 3/04527G

Received 28th July 1993

Accepted 18th October 1993